CNT Spin Qubit and Its Development

Internship Report M2 QLMN

Supervisor: Quentin Schaeverbeke

Xitian Huang

April - August 2024

Contents

1 Introduction

This report summarises the theoretical work being done in this internship at C12. It is divided into several parts. In Section 1, the carbon nanotube based spin qubit developed at C12 is introduced. Its Hamiltonian and quantum gates are derived. In Section 2, a permutation representation is formulated to find the unitary operator for a two-qubit swap gate, taking into account the effect of idle qubits. In Section 3, a tensor network method is developed to make the quantum simulation more efficiently.

1.1 Spin Qubit

The pursuit for best qubit with high fidelity and low decoherence is one of the most important subjects of making a practical fault-tolerant quantum computer. At C12, the carbon nanotube is used as the host material for making a spin qubit on a silicon chip. The small nuclear spin of carbon atoms makes it a good candidate to avoid spin relaxation. The short range interaction between neighbouring qubits is circumvented by using microwave resonators, which also allows the long range interaction between qubits for the purpose of quantum gates. To realize a spin qubit, we choose a double quantum dot that allows us to trap one single electron with the effect of *Coulomb blockade* [1], which occurs when the temperature is low enough that the energy required to charge the junction is much higher than the thermal energy of the charge carriers. As a result, there is an increase in resistance under a small bias voltage on the quantum dot.

The Hamiltonian of electrons in a nanocircuit is [2] ($\hbar = 1$)

$$\hat{H}_{\text{tot}} = \int d^3 r \psi^\dagger(\vec{r}) \hat{h}_T(\vec{r}) \psi(\vec{r}) + \hat{H}_{\text{Coul}} + \omega_c \hat{a}^\dagger \hat{a} \tag{1}$$

where the field operator $\psi(\vec{r})$ describes all the tunnelling electrons in the nanocircuit, $\hat{H}_{\text{Coul}}$ is Coulomb interaction between tunnelling electrons and can be ignore since there is only one single electron in our case. $\hbar\omega_0 \hat{a}^\dagger \hat{a}$ is the cavity mode of resonator. In particular, the single electron Hamiltonian is

$$\hat{h}_T(\vec{r}) = \frac{1}{2m}\left(\frac{1}{i}\vec{\nabla}_r + e\vec{A}(\vec{r})\right)^2 - e\Phi_{\text{harm}}(\vec{r}) - eV_{\text{conf}}(\vec{r}) + \mu\vec{B}(\vec{r}) \cdot \vec{S} \tag{2}$$

where $e, \mu, m, \vec{S}$ are electron charge, Bohr magneton, electron mass and Pauli vector respectively. A magnetic field $\vec{B}$ is applied on the nanocircuit and $\vec{A}$ is its vector potential. Φ_{harm} is the potential due to DC voltage on the circuit gates and V_{conf} is the potential confining the electron in the circuit. We will ignore the weak coupling between a single spin and the magnetic field. Defects in the carbon nanotube will give rise to inter-valley coupling and is neglected here as well. Ferromagnetic contact is used for the generation of inhomogeneous magnetic fields, since a non-colinear contact gives spin polarization of electric current. From this, along with knowledge of band structure of carbon nanotube, it is found that the effective Hamiltonian describing the single electron in the carbon nanotube based double quantum dot is [3]

$$H_e = \frac{\varepsilon}{2}\tau_z + \gamma\tau_x + \frac{\alpha_{as}}{2}\sigma_x\tau_z + \frac{\alpha_s}{2}\sigma_z, \tag{3}$$

where α_{as}, α_s are the anti-symmetric and symmetric components of spin magnetic field interaction, τ_z, τ_x and σ_z, σ_x are Pauli operators of electron's orbitals and spins. Hence

it is in the product space of position and spin. ε and γ are the chemical potential and tunnelling rate between the dots. We will control these parameters so that only 2 states of the 4 will become the basis states of the spin qubit.

We now proceed to the exact diagonalization of this Hamiltonian to obtain the energy eigenstates. Before that, it is useful to be reminded of some usual quantum mechanics.

Definition 1 (Pauli Matrices)**.**

$$I = \begin{bmatrix} 1 & 0 \\ 0 & 1 \end{bmatrix} \quad \sigma_x = \begin{bmatrix} 0 & 1 \\ 1 & 0 \end{bmatrix} \quad \sigma_y = \begin{bmatrix} 0 & -i \\ i & 0 \end{bmatrix} \quad \sigma_z = \begin{bmatrix} 1 & 0 \\ 0 & -1 \end{bmatrix}$$
$$\sigma_+ = \begin{bmatrix} 0 & 1 \\ 0 & 0 \end{bmatrix} \quad \sigma_- = \begin{bmatrix} 0 & 0 \\ 1 & 0 \end{bmatrix}$$
$$\sigma_\pm = \frac{\sigma_x \pm i\sigma_y}{2}$$

$\{I, \sigma_x, \sigma_y, \sigma_z\}$ forms a basis for the vector space of 2×2 Hermitian matrices over $\mathbb{R}$. Direct verification shows that they have the following relations:

$$\begin{aligned} \sigma_k^2 &= I & \sigma_+^2 &= \sigma_-^2 = 0 \\ [\sigma_j, \sigma_k] &= 2i\varepsilon_{jkl}\sigma_l & [\sigma_+, \sigma_-] &= \sigma_z \\ \{\sigma_j, \sigma_k\} &= 2\delta_{jk} I & \{\sigma_+, \sigma_-\} &= 0 \end{aligned} \tag{4}$$

These will come handy in many of the subsequent calculations. Conventionally, τ is usually used for orbital Pauli operator and σ for spins.

Theorem 2 (Spectral Theorem (Decomposition) [4])**.** Let A be a linear operator on a finite dimensional inner product space V, then the following are equivalent

1. A is a normal operator ($A^\dagger A = AA^\dagger$)
2. A is unitarily diagonalizable: $\exists$ unitary U such that $UAU^\dagger = \Sigma$ and Σ is diagonal.

Furthermore, if A is normal, then there exist linear operators $E_1, \ldots, E_r$ on V and scalars $\lambda_1, \ldots, \lambda_r$ such that

$$\begin{aligned} T &= \sum_{i=1}^{r} \lambda_i E_i, & \sum_{i=1}^{r} E_i &= I \\ E_i^2 &= E_i & &\text{projective} \\ E_i E_j &= 0 (i \neq j) & &\text{orthogonal projection} \end{aligned} \tag{5}$$

In quantum mechanics, operators of observables are Hermitian and thus normal. Examples of such decomposition are Hamiltonian in terms of its eigenstates $H = \sum_E |E\rangle\langle E|$ and density matrix $\rho = \sum_i p_i |i\rangle\langle i|$. Below is a very simple example of applying spectral decomposition.

Example 3. Exponential of Pauli operator is

$$e^{i\theta \hat{n}\cdot\vec{\sigma}} = I\cos\theta + i\sin\theta(\hat{n}\cdot\vec{\sigma}), \tag{6}$$

where $\hat{n} \in \mathbb{R}^3$ is a unit vector and $\vec{\sigma} = (\sigma_x, \sigma_y, \sigma_z)$.

Proof. This can be approached in two different ways. 1. Expand the exponential function as

$$e^{i\theta\hat{n}\cdot\vec{\sigma}} = \sum_{k=0}^{\infty} \frac{(i\theta)^k(\hat{n}\cdot\vec{\sigma})^k}{k!} \tag{7}$$

Since

$$\begin{aligned}(\hat{n}\cdot\vec{\sigma})^2 = \left(\sum_{i=1}^{3} n_i\sigma_i\right)^2 &= \sum(n_i\sigma_i)^2 + \sum_{i<j} n_i n_j\{\sigma_i,\sigma_j\} \\ &= \sum n_i^2 + 0 = 1,\end{aligned} \tag{8}$$

we have, for $k \in \mathbb{N}$,

$$(\hat{n}\cdot\vec{\sigma})^{2k} = I, \quad (\hat{n}\cdot\vec{\sigma})^{2k+1} = \hat{n}\cdot\vec{\sigma}. \tag{9}$$

Hence

$$\begin{aligned}e^{i\theta\hat{n}\cdot\vec{\sigma}} &= \sum_{k=0}^{\infty} \frac{(-1)^k\theta^{2k}}{(2k)!} I + \frac{i(-1)^k\theta^{2k+1}}{(2k+1)!}\hat{n}\cdot\vec{\sigma} \\ &= I\cos\theta + i\sin\theta\ \hat{n}\cdot\vec{\sigma}. \qquad \square\end{aligned} \tag{10}$$

2. A quicker way is to notice that $\hat{n}\cdot\vec{\sigma}$ is Hermitian and one can apply spectral decomposition on it. As a result, there exists eigenvectors $|\psi_1\rangle, |\psi_2\rangle$ of $\hat{n}\cdot\vec{\sigma}$ such that

$$\hat{n}\cdot\vec{\sigma} = \lambda_1|\psi_1\rangle\langle\psi_1| + \lambda_2|\psi_2\rangle\langle\psi_2|, \tag{11}$$

where λ_1, λ_2 are of values ± 1 by finding the determinant. Consequently,

$$\begin{aligned}e^{i\theta\hat{n}\cdot\vec{\sigma}} &= e^{i\theta(|\psi_1\rangle\langle\psi_1| - |\psi_2\rangle\langle\psi_2|)} \\ &= e^{i\theta}|\psi_1\rangle\langle\psi_1| + e^{-i\theta}|\psi_2\rangle\langle\psi_2| \\ &= \cos\theta \underbrace{(|\psi_1\rangle\langle\psi_1| + |\psi_2\rangle\langle\psi_2|)}_{I} + i\sin\theta \underbrace{(|\psi_1\rangle\langle\psi_1| - |\psi_2\rangle\langle\psi_2|)}_{\hat{n}\cdot\vec{\sigma}} \\ &= I\cos\theta + i\sin\theta\ \hat{n}\cdot\vec{\sigma}\end{aligned} \tag{12}$$

$\square$

Let us now examine the first two τ terms of H_e. It can be expressed as

$$H_0 = \frac{\varepsilon}{2}\tau_z + \gamma\tau_x = \frac{1}{2}\begin{bmatrix}\varepsilon & 2\gamma \\ 2\gamma & -\varepsilon\end{bmatrix} = \frac{\Omega}{2}\begin{bmatrix}\cos\theta & \sin\theta \\ \sin\theta & -\cos\theta\end{bmatrix} \tag{13}$$

where $\Omega = \sqrt{\varepsilon^2 + 4\gamma^2}$ and $\tan\theta = 2\gamma/\varepsilon$. The basis transformation can be found as

$$U_1 = \begin{bmatrix}\cos\frac{\theta}{2} & -\sin\frac{\theta}{2} \\ \sin\frac{\theta}{2} & \cos\frac{\theta}{2}\end{bmatrix} = e^{-i\frac{\theta}{2}\tau_y}. \tag{14}$$

Hence in the new basis,

$$H_e = \frac{\Omega}{2}\tilde{\tau}_z + \frac{\alpha_s}{2}\sigma_z + \frac{\alpha_{as}}{2}\sigma_x(\cos\theta\tilde{\tau}_z - \sin\theta\tilde{\tau}_x) \tag{15}$$

where the tilde sign indicates the operator is in the new diagonal basis. We can do the exact same transformation on σ terms with

$$U_z = e^{-i\frac{\phi}{2}\tilde{\tau}_z\sigma_y}, \text{ and so } H_e = \frac{\Omega}{2}\tilde{\tau}_z + \frac{A}{2}\tilde{\sigma}_z - \frac{\alpha_{as}\sin(\theta)}{2}\tilde{\tau}_x\tilde{\sigma}_x \tag{16}$$

where $A = \sqrt{\alpha_s^2 + \alpha_{as}^2\cos^2\theta}$ and $\tan\phi = \alpha_{as}\cos\theta/\alpha_s$. Similar structure can be found by decomposing the Pauli operators into raising and lowering operators. With one more transformation, we will have in the end, the fully diagonalised Hamiltonian

$$H_e = \frac{\varepsilon_-}{2}\sigma_z + \frac{\varepsilon_+}{2}\tau_z \tag{17}$$

where $\varepsilon_\pm = \sqrt{(\Omega + A)^2 + \alpha_{as}^2\sin^2\theta} \pm \sqrt{(\Omega - A)^2 + \alpha_{as}^2\sin^2\theta}$. Physically, $\varepsilon_\sigma \equiv \varepsilon_-$ is the frequency of spin transition and $\varepsilon_\tau \equiv \varepsilon_+$ is the frequency of orbital transition. Due to the presence of charge noise from the nanocircuit, it is found that the optimal parameters for a robust control of qubits and low noise susceptibility should be

$$\begin{aligned} 2\gamma\alpha_s &= \alpha_{as}^2 + \alpha_s^2 \\ \varepsilon &= 0. \end{aligned} \tag{18}$$

When ε is big, we can isolate the state of qubit and turn it off as the *quantum memory*.

1.2 Two-Qubit Gate

To perform quantum operation requires putting the qubit inside a cavity, which generates the spin-photon coupling:

$$H_d = g_c\tau_z(a + a^\dagger), \tag{19}$$

where g_c is electric dipole coupling strength between the electron and a cavity photon. When transformed to the diagonalised basis and set $\varepsilon = 0$, this becomes

$$H_d = (g_\sigma\tau_z\sigma_x + g_\tau\tau_x)(a + a^\dagger) \tag{20}$$

where $g_\square$ are coupling constants obtained from measurement. The quantum state operation is thus realised by a photon-mediated coupling via an exchange of photon in the cavity that enables coherent long range interaction between two electrons. Then we have the full Hamiltonian for the two qubits,

$$H = H_0 + H_d \tag{21}$$

where

$$H_0 = \sum_{i=1,2}\frac{\varepsilon_\sigma}{2}\sigma_z^i + \frac{\varepsilon_\tau}{2}\tau_z^i + \omega_c a^\dagger a \tag{22}$$

$$H_d = \sum_{i=1,2}\left(g_\sigma\tau_z^i\sigma_x^i + g_\tau\tau_x^i\right)(a + a^\dagger) \tag{23}$$

Superscript i denotes the two qubits 1 and 2. The eigenstates of this new Hamiltonian may be found via the following perturbation approach in the dispersive regime, which isolates the higher orders of H_d and eliminates to first order. To do so let us introduce the following.

Theorem 4 (Baker-Hausdorff formula [5])**.** This theorem concerns the addition of the exponential function for non-commuting variables. Let X, Y be free generators of an associative ring R. Then

$$e^{-X} Y e^{X} = \sum_{l=0}^{\infty} \frac{[Y, X^l]}{l!} \tag{24}$$

where the l-fold iterated commutator is

$$[Y, X^l] = [\ldots, [[Y, X], X] \ldots X]. \tag{25}$$

Definition 5 (Schrieffer-Wolff Transformation [6])**.** There exists a unitary transformation S on $H = H_0 + H_d$ such that $\bar{H} = e^S H e^{-S}$ has no terms in the first order in H_d. We can write, after expanding with the Baker-Hausdorff formula, that

$$\bar{H} = H_0 + \underbrace{H_d + [S, H_0]}_{=0} + \underbrace{[S, H_d] + \frac{1}{2}[S, [S, H_0]]}_{=\frac{1}{2}[S, H_d]} + \ldots \tag{26}$$

Therefore we only need to find S such that $[H_0, S] = H_d$.

S can be found by assuming $S = S_+ a - S_- a^\dagger$ and plug in Pauli matrices in S_+, S_- as an ansatz. Back to our original analysis of the Hamiltonian, in the *resonant regime* when the frequency of spin transition is equal to the cavity mode, i.e., $\varepsilon_\sigma = \omega_c$, there is a collectively enhanced two-qubit coupling [7] via exchange of real photons. Here we will be going into the *dispersive regime* where photon frequency is detuned from the qubit spin transition frequency and the coherent long range interaction is mediated by the exchange of virtual photons. If the coupling strength is small enough that $g_{\tau(\sigma)} \ll |\varepsilon_{\tau(\sigma)} - \omega_c|$, we can use the Schrieffer-Wolff transformation to decouple the spin subspaces from the cavity to first order. Therefore the suitable regime of operating is when $\omega_c \approx \varepsilon_\sigma$, and

$$\frac{g_\tau |\Delta|}{|\varepsilon_\tau - \omega_c|} \ll g_\sigma \ll |\Delta| \tag{27}$$

where the detuning $\Delta = \varepsilon_\tau - \omega_c$. Assume the two qubits are identical and an empty cavity $\langle a^\dagger a \rangle = 0$, by the previous mentioned transformation and to the first order of g_σ / Δ, the Hamiltonian transforms to [8]

$$\bar{H} = \sum_{i=1,2} \frac{\varepsilon_\tau}{2} \tau_z^i + \frac{\varepsilon_\sigma + g_\sigma^2/\Delta}{2} \sigma_z^i + \frac{g_\sigma g_\tau}{2\Delta} \sigma_y^i \tau_y^i + \frac{g_\sigma^2}{\Delta} \sigma_x^1 \sigma_x^2 \tau_z^1 \tau_z^2. \tag{28}$$

With a *rotating-wave approximation* at frequency ε_σ to ignore the non-resonant terms, it becomes

$$\bar{H} = \sum_{i=1,2} \frac{\varepsilon_\tau}{2} \tau_z^i + \frac{\varepsilon_\sigma + g_\sigma^2/\Delta}{2} \sigma_z^i + \frac{g_\sigma^2}{\Delta} (\sigma_+^1 \sigma_-^2 + \sigma_-^1 \sigma_+^2) \tau_z^1 \tau_z^2. \tag{29}$$

Hence the two-qubit gate Hamiltonian is

$$S = \gamma (\sigma_+^1 \sigma_-^2 + \sigma_-^1 \sigma_+^2). \tag{30}$$

Its time evolution is unitary operator

$$U_S = \begin{bmatrix} 1 & 0 & 0 & 0 \\ 0 & \cos(\gamma t) & -i\sin(\gamma t) & 0 \\ 0 & -i\sin(\gamma t) & \cos(\gamma t) & 0 \\ 0 & 0 & 0 & 1 \end{bmatrix} \tag{31}$$

which turns into an iSWAP gate at gate times $t = (4k+1)\frac{\pi}{2\gamma}$ for integer k. The performance of such gate may be affected by three sources of decoherence and infidelity. First, the full Hamiltonian contains the long distance orbital τ coupling, spin-orbital $\sigma - \tau$ coupling in the same qubit and between qubits. Second, the charge fluctuation in the semiconductor nanostructure can make the spin qubits susceptible to charge noise even for material with low magnetic noise. Third, the damping of the cavity contributes to decoherence as well.

2 Cross-talk Error

To describe the cross-talk error for a two qubit iSWAP gate, the following two Hamiltonians S and H are used. Suppose the system is composed of n qubits, 2 of which are active and the rest $n-2$ are idle qubits (See Fig. 1). Then S is the Hamiltonian for the two (active) qubit gate and H is the cross-talk Hamiltonian describing the weaker coupling between the two active qubits and idle qubits:

$$S = \sigma_+^1\sigma_-^2 + \sigma_-^1\sigma_+^2, \tag{32}$$

$$H = \sum_{i=1,2}\sum_{j=3}^{n}(\sigma_+^i\sigma_-^j + \sigma_-^i\sigma_+^j). \tag{33}$$

The superscript index ranges from 1 to n and denotes which qubit the operator acts on. If an index does not appear, the identity operator $\mathbb{1}$ is implied. For instance,

$$\sigma_+^1\sigma_-^2 \equiv \sigma_+^1 \otimes \sigma_-^2 \otimes \mathbb{1}^3 \otimes \ldots \otimes \mathbb{1}^n. \tag{34}$$

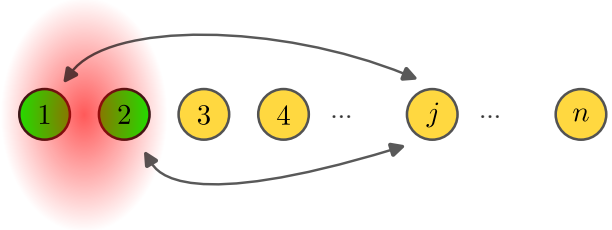

Figure 1: Two active qubits $1, 2$ talking with one of the idle qubits j.

Close examination on S and H suggests that they are merely permutations between qubits because of the raising and lowering Pauli operators. This is evident by the following reasoning. When they operate on one qubit,

$$\begin{aligned} \sigma_+|0\rangle &= |1\rangle \qquad & \sigma_-|0\rangle &= 0 \\ \sigma_+|1\rangle &= 0 \qquad & \sigma_-|1\rangle &= |0\rangle. \end{aligned} \tag{35}$$

Therefore for two qubits,

$$\sigma_+^i\sigma_-^j \cdot \begin{array}{l} |00\rangle = 0 \\ |01\rangle = |10\rangle \\ |10\rangle = 0 \\ |11\rangle = 0 \end{array} \qquad \sigma_-^i\sigma_+^j \cdot \begin{array}{l} |00\rangle = 0 \\ |01\rangle = 0 \\ |10\rangle = |01\rangle \\ |11\rangle = 0. \end{array} \tag{36}$$

As a result, both S and H permute the corresponding two qubits i, j and send other basis kets to 0. Based on this, we shall look at the effects of S, H on any general state to derive their algebraic properties.
Any pure state of n qubits in Hilbert space $\mathcal{H}_2^{\otimes n}$ can be represented by the following linear combination of tensor products in the orthonomal basis,

$$|\Psi\rangle = \sum_{i_k} \alpha_{i_1 i_2 \ldots i_n} \bigotimes_{k=1}^{n} |i_k\rangle = \sum_{i_1 i_2 \ldots i_n} \alpha_{i_1 i_2 \ldots i_n} |i_1 i_2 \ldots i_n\rangle, \tag{37}$$

where $i_k \in \{0, 1\}\ \forall k \in \mathbb{N}$, since each qubit has only two energy eigenstates denoted by $|0\rangle$ and $|1\rangle$. $\alpha_{i_1 i_2 \ldots i_n}$ are the complex coefficients and there are 2^n of them.

2.1 Permutation Symmetry

The idle qubit j we considered in Eq.(33) interacts only with active qubits $i = 1, 2$. Therefore, following the principle of mathematical induction, any conclusion on j extends to all $j \in \{3, \ldots n\}$ and effectively we need only to consider three qubits $1, 2, j$. Hence, the above general state *full representation* can be reduced to 8 terms only (*reduced representation*):

$$|\Psi\rangle = a_1|000\rangle + a_2|001\rangle + a_3|010\rangle + a_4|011\rangle + a_5|100\rangle + a_6|101\rangle + a_7|110\rangle + a_8|111\rangle, \tag{38}$$

where the first two terms in the ket are two active qubits and the third is the idle qubit. Note that the reduced representation still denotes a general n qubit state once a clear definition of the state vector and coefficient is given. For instance, one can define the second basis state

$$\begin{aligned} a_2|001\rangle &\equiv \sum_{u,v} a_2(u, v)\ |00u1v\rangle, \\ \text{where } |u\rangle &:= |u_1 u_2 \ldots u_r\rangle, u_i \in \{0, 1\}, \\ |v\rangle &:= |v_1 v_2 \ldots v_s\rangle, v_i \in \{0, 1\}, \\ r + s &= n - 3, \end{aligned} \tag{39}$$

and the other basis states will follow. The key point is that instead of being a constant, the coefficient here is a function that incorporates the information from other qubits. To simplify the notation, we denote the state as an ordered list of coefficients

$$|\Psi\rangle = (a_1, a_2, a_3, a_4, a_5, a_6, a_7, a_8).$$

Thus, using the relation in Eq.(36), one obtains,

$$\begin{aligned} S|\Psi\rangle &= (0, 0, a_5, a_6, a_3, a_4, 0, 0) \\ H|\Psi\rangle &= (0, a_3 + a_5, a_2, a_7, a_2, a_7, a_4 + a_6, 0). \end{aligned} \tag{40}$$

The matrix representations for them are the following two Hermitian matrices,

$$H = \begin{bmatrix} 0 & 0 & 0 & 0 & 0 & 0 & 0 & 0 \\ 0 & 0 & \mathbf{1} & 0 & \mathbf{1} & 0 & 0 & 0 \\ 0 & \mathbf{1} & 0 & 0 & 0 & 0 & 0 & 0 \\ 0 & 0 & 0 & 0 & 0 & 0 & \mathbf{1} & 0 \\ 0 & \mathbf{1} & 0 & 0 & 0 & 0 & 0 & 0 \\ 0 & 0 & 0 & 0 & 0 & 0 & \mathbf{1} & 0 \\ 0 & 0 & 0 & \mathbf{1} & 0 & \mathbf{1} & 0 & 0 \\ 0 & 0 & 0 & 0 & 0 & 0 & 0 & 0 \end{bmatrix} \quad S = \begin{bmatrix} 0 & 0 & 0 & 0 & 0 & 0 & 0 & 0 \\ 0 & 0 & 0 & 0 & 0 & 0 & 0 & 0 \\ 0 & 0 & 0 & 0 & \mathbf{1} & 0 & 0 & 0 \\ 0 & 0 & 0 & 0 & 0 & \mathbf{1} & 0 & 0 \\ 0 & 0 & \mathbf{1} & 0 & 0 & 0 & 0 & 0 \\ 0 & 0 & 0 & \mathbf{1} & 0 & 0 & 0 & 0 \\ 0 & 0 & 0 & 0 & 0 & 0 & 0 & 0 \\ 0 & 0 & 0 & 0 & 0 & 0 & 0 & 0 \end{bmatrix}. \quad (41)$$

Obviously, these two matrices can be reduced to lower dimension in block form as

$$H = \begin{bmatrix} 0 & \sigma_- & \sigma_- & 0 \\ \sigma_+ & 0 & 0 & \sigma_- \\ \sigma_+ & 0 & 0 & \sigma_- \\ 0 & \sigma_+ & \sigma_+ & 0 \end{bmatrix} \quad S = \begin{bmatrix} 0 & 0 & 0 & 0 \\ 0 & 0 & \mathbb{1} & 0 \\ 0 & \mathbb{1} & 0 & 0 \\ 0 & 0 & 0 & 0 \end{bmatrix}. \quad (42)$$

S can be seen as a transposition in the subspace. One can also start from Eq.(34) only, and write out the matrices of tensor products to get the same block matrices. However, the aforementioned argument is more rigorous and concise.

Beware that this matrix representation is only defined with respect to the reduced representation of qubit state in Eq.(38). However, it turns out that the block form in Eq.(42) is also valid in the full representation. Because only a fixed permutation is needed to convert between reduced and full representation of qubit state, i.e., there exists a set of u, v, u', v' such that $|00u1v\rangle = |00u'0v'\rangle$. Similarly for $|01\rangle, |10\rangle, |11\rangle$, which correspond to the four blocks in the block form representation. Due to the definition of parameters a_i in Eq.(39), the block form of H should be changed to a more general form for the full representation of the state as

$$H = \begin{bmatrix} 0 & M & M & 0 \\ N & 0 & 0 & M \\ N & 0 & 0 & M \\ 0 & N & N & 0 \end{bmatrix} \quad (43)$$

where M, N are square block matrices of dimension 2^{n-2} that account for all permutations of qubits and $M^\dagger = N$.

2.2 Algebraic Properties

Matrix multiplication shows that

$$H^2 = \begin{bmatrix} 2MN & 0 & 0 & 2M^2 \\ 0 & \{M,N\} & \{M,N\} & 0 \\ 0 & \{M,N\} & \{M,N\} & 0 \\ 2N^2 & 0 & 0 & 2NM \end{bmatrix} \quad S^2 = \begin{bmatrix} 0 & 0 & 0 & 0 \\ 0 & \mathbb{1} & 0 & 0 \\ 0 & 0 & \mathbb{1} & 0 \\ 0 & 0 & 0 & 0 \end{bmatrix}. \quad (44)$$

Note that the non-zero entries of powers of H, H^2 don't change and $\det H = \det S = 0$. Hence they are not invertible. With this, we also find the following identities: $\forall\, k \in \mathbb{N}$,

$$\begin{aligned}
S^{2k+1} = S,\, S^{2k} = S^2 & \qquad \textit{powers of } S \\
S^2 H^k = S H^k & \qquad \textit{action of } S \textit{ on } H \textit{ is idempotent} \\
H^k S^2 = H^k S & \qquad \textit{action of } S \textit{ on } H \textit{ is idempotent} \\
S H^k + H^k S = H^k \quad k \text{ odd} & \qquad \textit{anti-commutator} \\
S H^k S = 0 \quad k \text{ odd} & \qquad \textit{sandwich rule} \\
[S, H^{2k}] = 0 & \qquad \textit{commutator}
\end{aligned} \tag{45}$$

It is easy to verify them with matrix algebra. For a more rigorous proof, induction suffices.

2.3 Non-Commutative Algebra

To find the unitary operator of the Hamiltonian $S + mH$, we need to exponentiate it. Since S and H do not commute, $e^{S+mH} \neq e^S e^{mH}$, special treatment involving non-commutative algebra is necessary. One may start with Baker-Campbell-Hausdorff formula, Magnus expansion [5], or Zassenhaus formula [9], all of which can be used to find the integral solution of a linear operator of a linear first order differential equation in the form of exponential operator and they are inter-connected. For instance, the Zassenhaus formula is described as follows.

Theorem 6 (*Zassenhaus formula*)**.** Let X, Y be the two generators in a free ring (a non-commutative polynomial ring). There exist uniquely determined elements C_n such that

$$\begin{aligned}
e^{X+Y} &= e^X e^Y e^{C_2} e^{C_3} \dots \\
\text{where } C_2 &= -\frac{1}{2}[X, Y] \\
C_3 &= -\frac{1}{3}[[X, Y], Y] - \frac{1}{6}[[X, Y], X] \\
C_n &= \frac{1}{n!}\left[\frac{\partial^n}{\partial \lambda^n}(e^{-\lambda^{n-1} C_{n-1}} \dots e^{-\lambda^2 C_2} e^{-\lambda Y} e^{-\lambda X} e^{\lambda(X+Y)})\right]_{\lambda=0}.
\end{aligned} \tag{46}$$

In lower order approximation with such formulism, the exponential operator hinders the problem that it magnifies the order of X and Y and the commutators are difficult to find. Here we turn to a different approach by introducing the non-commutative version of Binomial theorem.

Definition 7. Let A, B be elements of a non-commutative ring R with identity 1. Define operator d_A as

$$d_A(B) \equiv d_A B = [A, B] = AB - BA. \tag{47}$$

We then have the following propositions:

$$\begin{aligned}
A d_A(B) &= d_A A(B) && A \text{ commutes with } d_A \\
d_A(XY) &= (d_A X)Y + X(d_A Y) && d_A \text{ is a derivative on } R \\
(A - d_A)X &= XA \\
d_A d_B(C) + d_B d_C(A) + d_C d_A(B) &= 0 && \text{Jacobi identity}
\end{aligned} \tag{48}$$

Hence R is also a Lie algebra with d_A as the Lie bracket. We will then be able to prove the following with induction.

Theorem 8 (*non-commutative binomial theorem [10]*)**.**

$$(A+B)^n = \sum_{k=0}^{n} \binom{n}{k} (A + \boldsymbol{d_B})^k B^{n-k}. \tag{49}$$

The addition of operator d_B is what it differs from the usual commutative binomial theorem. When no variable follows after d_B, the identity 1 is assumed and $d_B 1 = 0$. The non-commutative part $(A + \boldsymbol{d_B})^k$ is found through a recursive relation,

$$\begin{gathered} (A + \boldsymbol{d_B})^k = A^k + D_k(B, A) \\ D_{k+1}(B, A) = d_B A^k + (A + d_B)\, D_k(B, A) \\ \text{with initial value } D_0(B, A) = 0. \end{gathered} \tag{50}$$

Corollary 9. It follows from the above theorem that

$$e^{A+B} = (e^A + \sum_{k=0}^{\infty} \frac{D_k}{k!}) e^B. \tag{51}$$

Proof.

$$\begin{aligned} e^{A+B} &= \sum_{n=0}^{\infty} \frac{1}{n!} (A+B)^n \\ &= \sum_{n=0}^{\infty} \frac{1}{n!} \sum_{k=0}^{n} \binom{n}{k} (A + d_B)^k B^{n-k} \\ &= \sum_{n=k}^{\infty} \sum_{k=0}^{\infty} \frac{A^k + D_k(B, A)}{k!(n-k)!} B^{n-k} \\ &= \sum_{n=k}^{\infty} \sum_{k=0}^{\infty} \left(\frac{A^k}{k!} + \frac{D_k(B, A)}{k!} \right) \frac{B^{n-k}}{(n-k)!} \\ &= \left(e^A + \sum_{k=0}^{\infty} \frac{D_k}{k!} \right) e^B. \end{aligned} \tag{52}$$

□

Compare this with the Zassenhaus formula in Eq.(46), this corollary provides new perspective of approaching the exponential of linear operators. We will now demonstrate its advantage with the two Hamiltonians we have been dealing with so far, S, H.

2.4 Unitary Operator

With Corollary 9, we only have to deal with the terms $D_k(S, H)e^S$ for the computation of e^{H+S}. Using the recursive relation, the first few terms of D_k are calculated with the

help of identities in Eq.(45), keeping in mind that d_S commutes with e^S:

$$\begin{aligned}
D_0 &= 0 \\
D_1 &= 0 \\
D_2 &= d_S H \\
D_3 &= H d_S H + H \\
D_4 &= 2 d_S H^3 + H^2 + d_S H \\
D_5 &= 2 H d_S H^3 + 3 H^3 + H d_S H + H \\
D_6 &= 3 d_S H^5 + 3 H^4 + 4 d_S H^3 + H^2 + d_S H \\
D_7 &= 3 H d_S H^5 + 6 H^5 + 4 H d_S H^3 + 5 H^3 + H d_S H + H \\
D_8 &= 4 d_S H^7 + 6 H^6 + 10 d_S H^5 + 5 H^4 + 6 d_S H^3 + H^2 + d_S H \\
D_9 &= 4 H d_S H^7 + 10 H^7 + 10 H d_S H^5 + 15 H^5 + 6 H d_S H^3 + 7 H^3 + H d_S H + H. \qquad (53)
\end{aligned}$$

We have also used the following equalities to make the calculation simpler. For positive odd number α,

$$\begin{aligned}
d_S^2 H^\alpha &= H^\alpha \\
d_S H d_S H^\alpha &= 0 \\
H^2 d_S H^\alpha &= d_S H^{\alpha+2}. \qquad (54)
\end{aligned}$$

The terms D_k are arranged in decreasing orders of H and centred in the middle intentionally. Considering only the coefficients, it is reminiscent of Pascal's triangle (also known by many other names in other parts of the world) in which each number is a binomial coefficient with respect to its position in the triangle:

$$\begin{array}{ccccccccccc}
 & & & & & 1 & & & & & \\
 & & & & 1 & & 1 & & & & \\
 & & & 1 & & 2 & & 1 & & & \\
 & & 1 & & 3 & & 3 & & 1 & & \\
 & 1 & & 4 & & 6 & & 4 & & 1 & \\
1 & & 5 & & 10 & & 10 & & 5 & & 1 \\
 & 1 & & 6 & & 15 & & 20 & & 15 & & 6 & & 1 & \\
 & & 1 & & 7 & & 21 & & 35 & & 35 & & 21 & & 7 & & 1 \\
 & & & 1 & & 8 & & 28 & & 46 & & 70 & & 46 & & 28 & & 8 & & 1
\end{array}$$

Hence we can express D_k in terms of the binomial coefficients. The following coloured Figure 2 shows the correspondence between coefficients of D_k and binomial numbers of Pascal's triangle in a *stair-like* path.

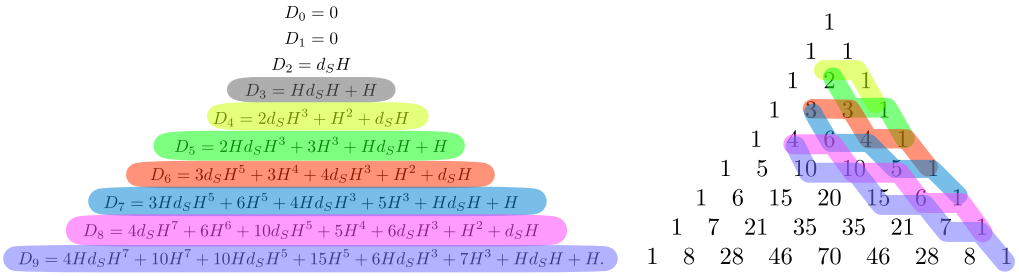

Figure 2: Correspondence between D_k coefficients and the stair-like paths in Pascal's triangle.

Example 10. Let $n \geq 2$ be an even number. D_n has the form

$$D_n = \binom{\frac{n}{2}}{1} d_S H^{n-1} + \binom{\frac{n}{2}}{2} H^{n-2} + \binom{\frac{n}{2}+1}{3} d_S H^{n-3} + \binom{\frac{n}{2}+1}{4} H^{n-4} + \dots$$
$$+ \binom{n-2}{n-3} d_S H^3 + \binom{n-2}{n-2} H^2 + \binom{n-1}{n-1} d_S H$$

$$D_{n+1} = \binom{\frac{n}{2}}{1} H d_S H^{n-1} + \binom{\frac{n}{2}+1}{2} H^{n-1} + \binom{\frac{n}{2}+1}{3} H d_S H^{n-3} + \binom{\frac{n}{2}+2}{4} H^{n-3} + \dots$$
$$+ \binom{n-1}{n-2} H^3 + \binom{n-1}{n-1} H d_S H + H$$

In summation notation,

$$D_n = \sum_{r=\frac{n}{2}}^{n-2} \binom{r}{2r-n+1} d_S H^{2n-2r-1} + \binom{r}{2r-n+2} H^{2n-2r-2} + d_S H$$

$$D_{n+1} = \binom{\frac{n}{2}}{1} H d_S H^{n-1} + \sum_{r=\frac{n}{2}+1}^{n-1} \binom{r}{2r-n} H^{2(n-r)+1} + \binom{r}{2r-n+1} H d_S H^{2(n-r)-1} + H$$

Similarly, we found that coefficients with the same order of H appearing in all the D_k follow along the diagonal of Pascal's triangle as shown in Fig. 3.

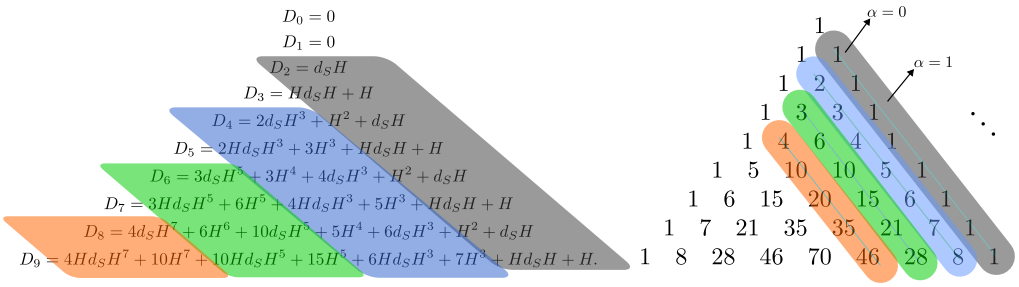

Figure 3: Correspondence between D_k coefficients of the same order in H and the diagonal of Pascal's triangle. Index α represents positions of recurrent terms of the same type.

Therefore, we can derive explicitly the sum of all $D_k(S,H)$ grouped in orders of H:

$$\begin{aligned}
\sum_{k=0}^{\infty} D_k(S,H) &= \sum_{n=2,4,\ldots}^{\infty} \sum_{\alpha=0}^{\infty} \binom{\frac{n}{2}+2\alpha}{1+2\alpha} (d_S H^{n-1} + H d_S H^{n-1}) + \binom{\frac{n}{2}+2\alpha+1}{1+2\alpha+1} (H^{n-1} + H^n), \\
\sum_{k=0}^{\infty} \frac{D_k(S,H)}{k!} &= \sum_{n=2,4,\ldots}^{\infty} \sum_{\alpha=0}^{\infty} \binom{\frac{n}{2}+2\alpha}{1+2\alpha} \left(\frac{d_S H^{n-1}}{(n+2\alpha)!} + \frac{H d_S H^{n-1}}{(n+2\alpha+1)!}\right) \\
&\quad + \binom{\frac{n}{2}+2\alpha+1}{1+2\alpha+1} \left(\frac{H^{n-1}}{(n+2\alpha+1)!} + \frac{H^n}{(n+2\alpha+2)!}\right) \equiv \sum_{n=2,4,\ldots}^{\infty} \mathcal{F}(n)
\end{aligned} \tag{55}$$

$n \in \{2, 4, 6, ...\}$ positive even number!

Meaning of index α is shown in Fig. 3. In combination of Corollary 9, we can get a full analytical expression of e^{S+H},

$$e^{S+H} = (e^H + \sum_{k=0}^{\infty} \frac{D_k}{k!}) e^S. \tag{56}$$

When $\|H^2\| \ll \|H\|$ and low-order approximation of order d is needed, simply do the summation of n in Eq.(55) up to d and expand e^H to the order d with:

$$\boxed{e^{S+H} \approx \left(1 + H + \frac{H^2}{2!} + \ldots + \frac{H^d}{d!} + \sum_{n=2,4,\ldots}^{d} \mathcal{F}(n)\right) e^S} \tag{57}$$

Going back to the original problem of finding the evolution operator, one has to consider also the coupling intensity γ, ratio m, and time dependence: $e^{-i\gamma t(S+mH)}$. Direct substitution of scalar m and $-i\gamma t$ as the coefficient of H into $\mathcal{F}(n)$ will work. However, S also carries scalar multiplier and replacing only S by $-i\gamma t S$ is incorrect because of the idempotent properties of S on H: higher orders of S are cancelled. Nevertheless, it is not difficult to extrapolate from the recursive relation in Eq.(50):

$$D_{k+1}(S,H) = d_S H^k + (H + d_S)\, D_k(S,H) \tag{58}$$

that the exponents of scalar on S and H add up to k, the index of D_k. Therefore,

$$\begin{aligned}
&\sum_{k=0}^{\infty} \frac{D_k(-i\gamma t S, -i\gamma t m H)}{k!} = \\
&\sum_{n=2,4,\ldots}^{\infty} \sum_{\alpha=0}^{\infty} \binom{\frac{n}{2}+2\alpha}{1+2\alpha} \left[\frac{(-i\gamma t)^{n+2\alpha}}{(n+2\alpha)!} d_S (mH)^{n-1} + \frac{(-i\gamma t)^{n+2\alpha+1}}{(n+2\alpha+1)!} m^n H d_S H^{n-1} \right] \\
&+ \binom{\frac{n}{2}+2\alpha+1}{1+2\alpha+1} \left[\frac{(-i\gamma t)^{n+2\alpha+1}}{(n+2\alpha+1)!} (mH)^{n-1} + \frac{(-i\gamma t)^{n+2\alpha+2}}{(n+2\alpha+2)!} (mH)^n \right] \\
&\equiv \sum_{n=2,4,\ldots}^{\infty} \mathcal{G}(n).
\end{aligned} \tag{59}$$

Hence for a full analytical expression of the unitary operator U,

$$\boxed{U = e^{-i\gamma t(S+mH)} = \left(e^{-i\gamma t m H} + \sum_{n=2,4,\ldots}^{\infty} \mathcal{G}(n) \right) U_S} \tag{60}$$

where $U_S = e^{-i\gamma t S}$.

For a second order approximation when $m \ll 1$, we can consider only $n = 2$:

$$\begin{aligned}
\mathcal{G}(2) = {} & m(\cos\gamma t - 1) d_S H + i m^2 (\gamma t - \sin\gamma t) H d_S H \\
& + i m (\gamma t - \sin\gamma t) H + m^2 (\cos\gamma t - 1 + \frac{(\gamma t)^2}{2}) H^2,
\end{aligned} \tag{61}$$

where the cos and sin terms are from the Taylor expansion. Finally, similar to Eq.(57):

$$U = e^{-i\gamma t(S+mH)} \approx \left[1 - i\gamma t m H - \frac{m^2(\gamma t)^2}{2} H^2 + \mathcal{G}(2) \right] e^{-i\gamma t S}$$

$$\boxed{U = \left[1 + (\cos\gamma t - 1)(m d_S H + m^2 H^2) - i \sin\gamma t \; mH + i(\gamma t - \sin\gamma t) \; m^2 H d_S H \right] U_S} \tag{62}$$

Setting the gate time $\gamma t = \frac{\pi}{2}(4k+1)$ for integer k, U_S becomes the iSWAP gate and

$$U = \left[1 - (i + d_S) mH - m^2 H^2 + i(\frac{\pi}{2} - 1) m^2 H d_S H \right] U_S. \tag{63}$$

3 Tensor Network

The simulation of quantum many body system requires enormous amount of computational power, this is especially true in the previous section on crosstalk from a large number of idle qubits on the quantum processor. A more efficient way of quantum computer simulation would be helpful. The large matrix we derived in the last Section is an example of computationally costly quantum operation. Gate decomposition could significantly reduce the cost of simulation and may help to increase the fidelity of the gates when decomposed in a fault-tolerant way. Theoretically its viability is demonstrated by Solovay-Kitaev theorem [11] which states that any set of quantum gates in SU(d) that generates a dense group in SU(d) can be used to approximate any quantum gate within a short circuit depth and such set can be found efficiently, thereby lays the foundation for finding universal quantum gates.

3.1 Gate Decomposition

Having obtained the two-qubit gate with error from idle qubits in Eq.(63), which we can express as,

$$U = \mathcal{L}(S, H)\, U_S \tag{64}$$

where $\mathcal{L}$ is a polynomial of S and to the second order of H and it should be close to unitary. Let us express U_S, H, S in Kronecker product notation to understand their actions on qubits:

$$U_S = \begin{bmatrix} 1 & 0 & 0 & 0 \\ 0 & 0 & -i & 0 \\ 0 & -i & 0 & 0 \\ 0 & 0 & 0 & 1 \end{bmatrix} \otimes \underbrace{I \otimes \cdots \otimes I}_{\#n}$$

$$S = \begin{bmatrix} 0 & 0 & 0 & 0 \\ 0 & 0 & 1 & 0 \\ 0 & 1 & 0 & 0 \\ 0 & 0 & 0 & 0 \end{bmatrix} \otimes \underbrace{I \otimes \cdots \otimes I}_{\#n}$$

$$\begin{aligned} H = &\sum_j \sigma_+ \otimes I \otimes \cdots \otimes \sigma_-^j \otimes \cdots \otimes I \\ &+ \sum_j \sigma_- \otimes I \otimes \cdots \otimes \sigma_+^j \otimes \cdots \otimes I \\ &+ \sum_j I \otimes \sigma_+ \otimes \cdots \otimes \sigma_-^j \otimes \cdots \otimes I \\ &+ \sum_j I \otimes \sigma_- \otimes \underbrace{\cdots \otimes \sigma_+^j \otimes \cdots \otimes I}_{\#n} \end{aligned} \tag{65}$$

I is the identity on one qubit. Apparently, U_S and S only operate on the first two active qubits, so they are easy to compute. H is more complicated to handle. Together with multiplication by S and coefficients from Eq.(59), $\mathcal{L}(S, H)$ becomes intricate to analyse. The goal here is to decompose it into a set of gates on a smaller number of qubits. Such decomposition significantly reduces the computational complexity of the simulation. Results from previous section which express the exponential of Hamiltonian in its ordered polynomial would be helpful for this decomposition.

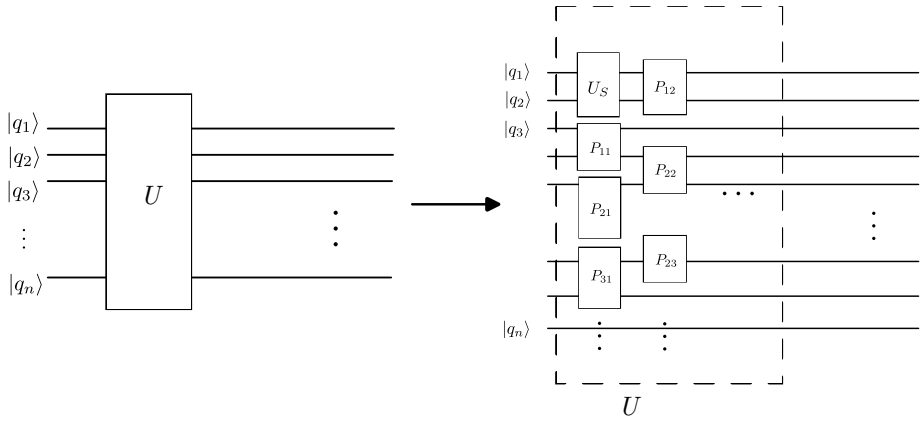

Figure 4: Decomposition of unitary operator U on n qubits into set of gates on smaller number of qubits.

Fig. 4 illustrates heuristically the decomposition on a n-qubit quantum circuit. We aim to decompose $\mathcal{L}$ into

$$\tilde{\mathcal{L}}(S,H) = \prod_{j=1}^{k} P_{1j} \otimes I^{\otimes a_{1j}} \otimes P_{2j} \otimes I^{\otimes a_{2j}} \otimes \cdots \otimes P_{dj} \otimes I^{\otimes a_{dj}} \tag{66}$$

In particular, $P_{11} = U_S$. Let $d = \lfloor \frac{n}{\ln n} \rfloor$, We can restrict $P_{ij} \in U(2^d)$ as the dimension of decomposed gates which acts on $\mathcal{H}_2^{\otimes d}$. k denotes the number of consecutive quantum gates. a_{ij} will be chosen explicitly. We will then apply a recursive algorithm so that in the end

$$\|\mathcal{L} - \tilde{\mathcal{L}}\|_F \leq C \tag{67}$$

where C is the threshold and $\|\cdot\|_F$ is the *Frobenius norm*, a measure of matrix that sums up squares of all entries.

Definition 11 (Frobenius norm)**.** For a $m \times n$ matrix over $\mathbb{C}$,

$$\|A\|_F = \sqrt{\sum_{i=1}^{m}\sum_{j=1}^{n} |a_{ij}|^2} = \sqrt{Tr(A^\dagger A)}. \tag{68}$$

Due to the invariant property of matrix trace, if the eigenvalues of A are σ_i, then

$$\|A\|_F = \sqrt{\sum_i |\sigma_i|^2}.$$

To decompose as Eq.(66), we present the following matrix related mathematics.

Theorem 12 (singular value decomposition SVD [4])**.** Given a rank-r, $n \times m$ matrix ($\in M_{n,m}$), let $q = \min\{m, n\}$. There exist unitary matrices $V \in M_n$ and $W \in M_m$ and

a square diagonal matrix with *singular values* on its diagonal

$$\Sigma_q = \begin{bmatrix} \sigma_1 & 0 & \cdots & 0 \\ 0 & \sigma_2 & \cdots & 0 \\ \vdots & \vdots & \ddots & \vdots \\ 0 & 0 & \cdots & \sigma_q \end{bmatrix} \tag{69}$$

such that $\sigma_1 \geq \sigma_2 \geq \cdots \geq \sigma_r \geq 0 = \sigma_{r+1} = \cdots = \sigma_q$ and $A = V\Sigma W^\dagger$, in which

$$\begin{aligned} &\Sigma = \Sigma_q \text{ if } m = n, \\ &\Sigma = \begin{bmatrix} \Sigma_q & 0 \end{bmatrix} \in M_{n,m} \text{ if } m > n, \\ &\Sigma = \begin{bmatrix} \Sigma_q \\ 0 \end{bmatrix} \in M_{n,m} \text{ if } n > m \end{aligned} \tag{70}$$

Definition 13 (low rank approximation [12])**.** We already know from the previous singular value decomposition that a rank-r matrix $A \in M_{n,m}$ can be factorised into $A = V\Sigma W^\dagger$, and hence

$$A = \sum_{i=1}^{q} \sigma_i \mathbf{v_i} \mathbf{w_i}^\dagger,$$

where $\mathbf{v_i}, \mathbf{w_i}$ are columns of V, W,

$$V = \begin{bmatrix} | & | & & | \\ \mathbf{v_1} & \mathbf{v_2} & \cdots & \mathbf{v_n} \\ | & | & & | \end{bmatrix} \qquad W = \begin{bmatrix} - & \mathbf{w_1}^\dagger & - \\ & \vdots & \\ - & \mathbf{w_2}^\dagger & - \end{bmatrix}$$

The low rank approximation of target rank k approximate A as

$$A_k = \sum_{i=1}^{k} \sigma_i \mathbf{v_i} \mathbf{w_i}^\dagger. \tag{71}$$

The singular values are sorted from big to small and only the first k of them are included. It has been shown that this approximation is optimal in terms of Frobenius norm, i.e.,

$$\forall A, B \in M_{n,m}, \quad rank(B) = k, \tag{72}$$

$$\|A - A_k\|_F \leq \|A - B\|_F \tag{73}$$

Low rank approximation is widely used in many areas of science. One modern example is large language model and its fine-tuning [13]. It offers compression of the matrix from $\mathcal{O}(mn)$ to $\mathcal{O}(k(m+n))$. We will now see how it can also be applied to the quantum computing regime as an application to the gate decomposition.

Example 14 (nearest Kronecker product problem)**.** The decomposition of gates into gates on smaller number of qubits is similar to a nearest Kronecker product problem (NKP). Suppose $A \in \mathbb{R}^{m \times n}$ and $m = m_1 m_2, n = n_1 n_2$, we want to minimize [14]

$$\phi(B, C) = \|A - B \otimes C\|_F \tag{74}$$

where $B \in \mathbb{R}^{m_1 \times n_1}, C \in \mathbb{R}^{m_2 \times n_2}$.

Theorem 15. First introduce the *vec* operator which stacks columns of a matrix to form a column vector. For instance $A = (a_{ij})$ and $B = vec(A)$ implies $a_{ij} = b_{i+m(j-1)}$. Then

$$\|A - B \otimes C\|_F^2 = \|\mathcal{R}(A) - vec(B) \otimes vec(C)\|_F^2 \tag{75}$$

$\mathcal{R}(A)$ is arranged so that equations are the same after vectorization of B, C.

Corollary 16. If $\mathcal{R}(A)$ has SVD that $A = V\Sigma W^\dagger$, then B, C defined by

$$vec(B) = \sqrt{\sigma_1}\mathbf{v_1} \qquad vec(C) = \sqrt{\sigma_1}\mathbf{w_1} \tag{76}$$

minimizes $\|A - B \otimes C\|_F^2$. Doing the reverse of *vec* gives B, C back to original matrix form. This is the best rank-1 approximation. For higher rank r, with

$$vec(B_k) = \sqrt{\sigma_k}\mathbf{v_k} \qquad vec(C_k) = \sqrt{\sigma_k}\mathbf{w_k} \tag{77}$$

$\sum_{k=1}^{r} \sigma_k B_k \otimes C_k$ is the closest matrix to A in Frobenius norm as the sum of r Kronecker products.

When either B or C is fixed, the problem becomes a least square problem. The structure of decomposed matrices remain the same (e.g. bandedness, symmetry, orthogonal, stochastic). Applying the above algorithm recursively solves Eq.(66):

$$\begin{aligned} A &= a_1 \otimes A_1 \\ A_1 &= a_2 \otimes A_2 \\ A_2 &= a_3 \otimes A_3 \\ &\vdots \\ A_{n-2} &= a_{n-1} \otimes A_{n-1} \end{aligned} \tag{78}$$

However, this recursive is not guaranteed to be optimal as it involves a series of Kronecker products. A more systematic way of decomposition called *higher order orthogonal iteration* (HOOI) exists. [15]. It finds the best rank approximation to $\mathcal{A} = \mathcal{B} \otimes \mathbf{U_1} \otimes \mathbf{U_2} \otimes \cdots \times \mathbf{U_n}$.

3.2 Matrix Product State

Recall that any pure state of n qubits $|\Psi\rangle \in \mathcal{H}_2^{\otimes n}$ is

$$|\Psi\rangle = \sum_{i_1 i_2 \ldots i_n} \alpha_{i_1 i_2 \ldots i_n} |i_1 i_2 \ldots i_n\rangle, \tag{79}$$

where $i_k \in \{0, 1\}\ \forall k \in \mathbb{N}$. There are 2^n number of coefficients $\alpha_{i_1 i_2 \ldots i_n}$. The exponential amount of parameters in such interacting quantum system makes it intractable. If quantum computers were to offer a speed-up compared to classical computer, then it must have dynamics that cannot be efficiently simulated. It turns out entanglement is one necessary but not sufficient condition for quantum computational advantage. The summation of i_k is where the entanglement between qubits comes from. As a result, we need a quantifying measure of entanglement [16]. We start with a *Schmidt decomposition* of $|\Psi\rangle$ on a partition $A : B$,

$$|\Psi\rangle = \sum_{\alpha=1}^{\chi_A} \lambda_\alpha |\Phi_\alpha^{[A]}\rangle \otimes |\Phi_\alpha^{[B]}\rangle \tag{80}$$

where $|\Phi_\alpha^{[A]}\rangle, |\Phi_\alpha^{[B]}\rangle$ are eigenvectors of reduced density matrix in the subsystems $\rho^{[A]}, \rho^{[B]}$ and λ_α is the Schmidt coefficient. The rank χ_A of $\rho^{[A]}$ is a natural measure between A and B. Since the partition $A:B$ is not unique,

$$\chi \equiv \max_A \chi_A$$

over all possible partition of n qubits quantifies the entanglement of $|\Psi\rangle$. The related entanglement measure

$$E_\chi \equiv \log_2(\chi)$$

will be used here. After the previous gate decomposition, a corresponding state decomposition is required so that we know how smaller gates act on smaller number of qubits. Coefficients of $|\Psi\rangle$ are decomposed as *matrix product state MPS*

$$\alpha_{i_1,i_2,\ldots,i_n} = \sum_{a_1,\ldots,a_{n-1}} \left(\Gamma^{[1]i_1}_{a_1}\lambda^{[1]}_{a_1}\right)\left(\Gamma^{[2]i_2}_{a_1a_2}\lambda^{[2]}_{a_2}\right)\left(\Gamma^{[3]i_3}_{a_2a_3}\lambda^{[3]}_{a_3}\right)\cdots\left(\Gamma^{[n-1]i_{n-1}}_{\alpha_{n-2}\alpha_{n-1}}\lambda^{[n-1]}_{a_{n-1}}\right)\Gamma^{[n]i_n}_{a_{n-1}} \tag{81}$$

where indices $i_l \in \{0,1\}$ and $\alpha_i \in \{1,2,\ldots,\chi\}$ run on n tensors Γ and $n-1$ vectors λ. Such product state is obtained from an iterative procedure of Schmidt decomposition and it depends on the specific ordering of the qubits. A tensor network notation in Fig. 5 visualises such decomposition more intuitively.

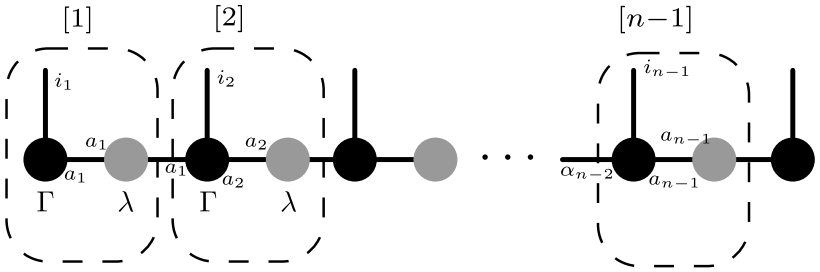

Figure 5: Tensor diagram notation of the matrix product state, indices are represented lines connecting the circles which represent a tensor or a vector. Summation is indicated by two lines connecting each other.

Index on connected lines is called band index. After the MPS decomposition, 2^n coefficients turn into around $n(2\chi^2+\chi) \sim n\exp(E_\chi)$ parameters. If E_χ scales as $\mathcal{O}(\log(n))$, only $poly(n)$ parameters are needed, leading to a more efficient way of simulation. Now let us look how quantum gates act on MPS.

Lemma 17 (one-qubit gate on MPS)**.** Unitary operation U on qubit l only modifies tensor $\Gamma^{[l]}$

$$\Gamma'^{i}_{\alpha\beta} = \sum_{j=0,1} U^i_j \Gamma^j_{\alpha\beta}, \quad \forall\alpha,\beta = 1,2,\ldots,\chi. \tag{82}$$

Taking into account of all matrices multiplication of U for all α,β, $\mathcal{O}(\chi^2)$ of basic operations is needed for one-qubit gate operation.

Lemma 18 (two-qubit gate on MPS)**.** Unitary operation V on two consecutive qubits l and $l+1$ only modifies $\Gamma^{[l]}, \lambda^{[l]}, \Gamma^{[l+1]}$ and this costs $\mathcal{O}(\chi^3)$ of basic operations.

If two qubit gate is not next to one another in order, swap gate is needed to bring them together.

4 Conclusion

In this report, we have introduced the Hamiltonian for a carbon nanotube based, photon mediated spin qubit in microwave resonator and found its exact diagonalization by a sequence of rotational transformation. The two-qubit quantum gate in the dispersive regime is found via a first order approximation. Subsequently we used these results to analyse the weak coupling between active and idle qubits on a many-qubit quantum processor, known as the crosstalk. Taking advantage of non-commutative algebra and permutation representation, we successfully derived a unitary quantum gate without resorting to any approximation technique. It expresses analytically in any order of Hamiltonian. This provides the basis for decomposing such high dimensional gate using SVD or HOOI which is readily compatible with a tensor network of quantum state representation and illuminates a way to efficient simulation of quantum error on the system as a whole. However the report has only outlined the fundamental theoretical framework. A more practical implementation and simulation are needed to quantify such method.

References

[1] C Livermore, CH Crouch, RM Westervelt, KL Campman, and AC Gossard. The coulomb blockade in coupled quantum dots. *Science*, 274(5291):1332–1335, 1996.

[2] Audrey Cottet, Takis Kontos, and Benoît Douçot. Electron-photon coupling in mesoscopic quantum electrodynamics. *Physical Review B*, 91(20):205417, 2015.

[3] Q. Schaeverbeke, W. Legrand, T. Kontos, and M. M. Desjardins. Carbon nanotube spin qubit. 2022.

[4] Roger A Horn and Charles R Johnson. *Matrix analysis*. Cambridge university press, 2012.

[5] Wilhelm Magnus. On the exponential solution of differential equations for a linear operator. *Communications on pure and applied mathematics*, 7(4):649–673, 1954.

[6] John R Schrieffer and Peter A Wolff. Relation between the anderson and kondo hamiltonians. *Physical Review*, 149(2):491, 1966.

[7] D. J. van Woerkom, P. Scarlino, J. H. Ungerer, C. Müller, J. V. Koski, A. J. Landig, C. Reichl, W. Wegscheider, T. Ihn, K. Ensslin, and A. Wallraff. Microwave photon-mediated interactions between semiconductor qubits. *Phys. Rev. X*, 8:041018, Oct 2018.

[8] Mónica Benito, Jason R Petta, and Guido Burkard. Optimized cavity-mediated dispersive two-qubit gates between spin qubits. *Physical Review B*, 100(8):081412, 2019.

[9] Masuo Suzuki. On the convergence of exponential operators—the zassenhaus formula, bch formula and systematic approximants. 1977.

[10] Walter Wyss. Two non-commutative binomial theorems, 2017.

[11] A Yu Kitaev. Quantum computations: algorithms and error correction. *Russian Mathematical Surveys*, 52(6):1191, 1997.

[12] Carl Eckart and Gale Young. The approximation of one matrix by another of lower rank. *Psychometrika*, 1(3):211–218, 1936.

[13] Edward J Hu, Yelong Shen, Phillip Wallis, Zeyuan Allen-Zhu, Yuanzhi Li, Shean Wang, Lu Wang, and Weizhu Chen. Lora: Low-rank adaptation of large language models. *arXiv preprint arXiv:2106.09685*, 2021.

[14] C. F. Van Loan and N. Pitsianis. *Approximation with Kronecker Products*, pages 293–314. Springer Netherlands, Dordrecht, 1993.

[15] Lieven De Lathauwer, Bart De Moor, and Joos Vandewalle. On the best rank-1 and rank-(r 1, r 2,..., rn) approximation of higher-order tensors. *SIAM journal on Matrix Analysis and Applications*, 21(4):1324–1342, 2000.

[16] Guifré Vidal. Efficient classical simulation of slightly entangled quantum computations. *Physical review letters*, 91(14):147902, 2003.

A Appendix

A.1 Numerical Implementation

Recall that the Hamiltonians for cross-talk error in a two-qubit gate with q idle qubits are

$$S = \sigma_+^1\sigma_-^2 + \sigma_-^1\sigma_+^2,$$
$$H = \sum_{i=1,2}\sum_{j=3}^{q+2}(\sigma_+^i\sigma_-^j + \sigma_-^i\sigma_+^j).$$

When q is big, the sizes of S and H increase exponentially like 2^{q+2}. and the number of entries is $2^{2(q+1)} = 4^{q+1}$. This will consume a big amount of memory to store them. Fortunately, we can reduce the memory usage. As discussed in Sections 2.1 and 2.2, the Hamiltonians exhibit different symmetrical properties and they are very sparse matrices:

$$H = \begin{bmatrix} 0 & M & M & 0 \\ N & 0 & 0 & M \\ N & 0 & 0 & M \\ 0 & N & N & 0 \end{bmatrix} \qquad S = \begin{bmatrix} 0 & 0 & 0 & 0 \\ 0 & 0 & \mathbb{1} & 0 \\ 0 & \mathbb{1} & 0 & 0 \\ 0 & 0 & 0 & 0 \end{bmatrix}$$

For S, it is trivial since it has two identity blocks, each of which has dimension 2^q, hence there are effectively only 2^{q+1} (non-zero) entries. For H, it is more complicated. To illustrate, we plotted H for different q in Fig. 6.

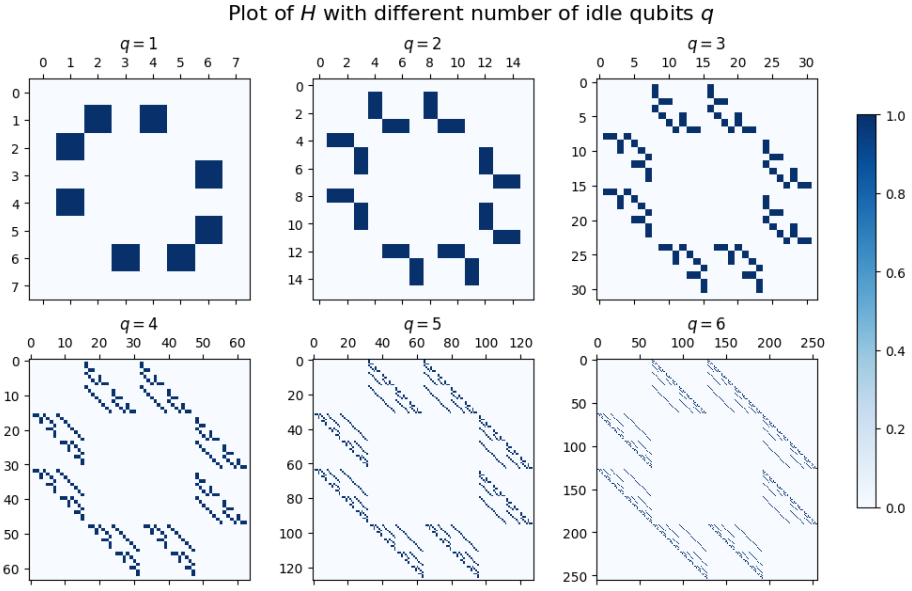

Figure 6: Plot of H as a matrix for different q. Notice the fractal structure as q increases.

When $q = 1$, the plot is exactly the matrix derived in Eq.(41). This is not surprising since our approach to it uses only 1 idle qubit. As q increases, each block has more

entries, but they all follow a pattern. In particular, it confirms that the block form is indeed correct and $M^\dagger = N$. It is found that the shape of block follows a fractal structure. One may see it more clearly in Fig. 7. We can formulate the non-zero entries in the fractal unit M as follows.

Coordinate in the matrix is represented by (x, y), where x, y are row and column number respectively. Define starting point set as

$$P_S = \left\{ p \in \mathbb{R}^{2^q \times 2^q} \,\middle|\, p = (2^n, 0) + k \cdot 2^{2^n+1}(1,1),\ \forall k \in \{0, 1, 2, \ldots, 2^{q-n-1} - 1\} \right\}, \quad (83)$$

where $n \in \{0, 1, 2, \ldots, q-1\}$ represents the $(n{+}1)$-th off-diagonal. There are q off-diagonals. Then diagonal point set representing every slice of continuous diagonal points is

$$P_D = \{ p = x + m \cdot (1,1) \,|\, x \in P_S,\ \forall m \in \{1, 2, \ldots, 2^n - 1\} \}. \quad (84)$$

Thus for each $(n{+}1)$-th off-diagonal, the non-zero entry point set is

$$P_n = P_S \cup P_D. \quad (85)$$

In this way, we no longer need to store all the 4^{q+1} entries but only those non-zeros and their coordinates and there are $4q \cdot 2^q$ of them. The memory usage is greatly reduced and simulation is more efficient.

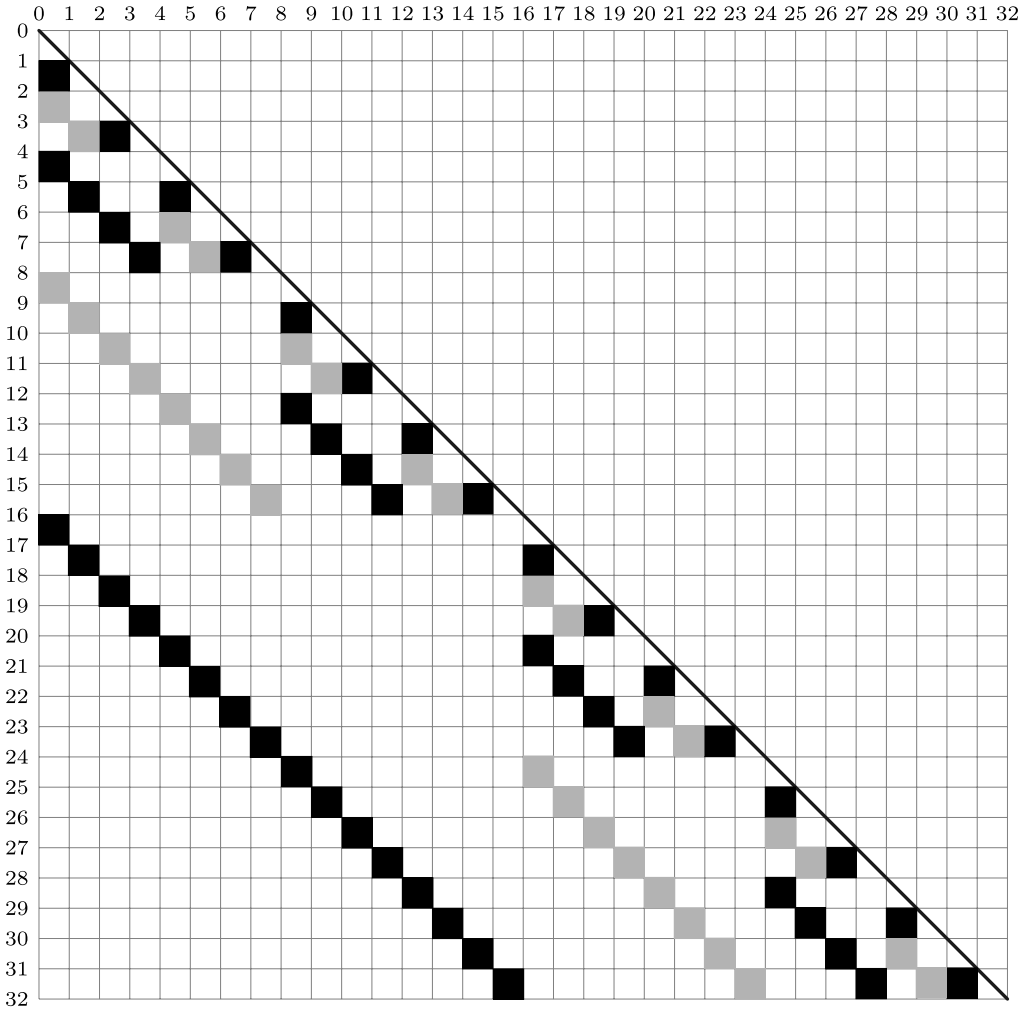

Figure 7: Visual representation of the fractal unit M in Hamiltonian H when number of idle qubits is 5. Grey and black colours are used to distinguish different off-diagonal entries. All coloured squares have value 1 and the rest are 0.

The following Python function returns H following the argument we described here.

```
import numpy as np
# need updated SciPy version (>=1.12.0) to use `block_array`
from scipy.sparse import coo_matrix, block_array, csr_array

def Hmatrix(q: int) -> csr_array:
  indices = []
  # create the fractal structured unit of the matrix
  for n in range(q):
    for k in range(2**(q-n-1)):
      begin_coo = (2**n + k * 2**(n+1), 0 + k * 2**(n+1))
      indices.append(begin_coo)
```

```
    if n != 0: # n=0 (1st off-diagonal) has no diagonal terms
        for m in range(1, 2**n):
          diag_coo = (begin_coo[0] + m, begin_coo[1] + m)
          indices.append(diag_coo)
# convert to a numpy array, two rows for two coordinates of the matrices.
idx_A = np.array(indices).T
# symmetrize along the diagonal (A transposed = B)
idx_B = idx_A[::-1]
A = coo_matrix(([1]*len(idx_A[0]), (idx_A[0],idx_A[1])),shape=(2**q,)*2)
B = coo_matrix(([1]*len(idx_B[0]), (idx_B[0],idx_B[1])),shape=(2**q,)*2)
# block form of the hamiltonian containing the units A & B
blocks = [[None, A, A, None],[B,None,None,A],[B,None,None, A],[None,B,B,None]]
mat = block_array(blocks)
return mat
```